A Convolutional Neural Network for Supernova Time-Series Classification

Helen Qu [1] **Masao Sako** [1] **Anais Möller** [2] **Cyrille Doux** [3]

Abstract

One of the brightest objects in the universe, supernovae (SNe) are powerful explosions marking the end of a star's lifetime. Supernova (SN) type is defined by spectroscopic emission lines, but obtaining spectroscopy is often logistically unfeasible. Thus, the ability to identify SNe by type using time-series image data alone is crucial, especially in light of the increasing breadth and depth of upcoming telescopes. We present a convolutional neural network method for fast supernova time-series classification, with observed brightness data smoothed in both the wavelength and time directions with Gaussian process regression. We apply this method to full duration and truncated SN time-series, to simulate retrospective as well as real-time classification performance. Retrospective classification is used to differentiate cosmologically useful Type Ia SNe from other SN types, and this method achieves $> 99\%$ accuracy on this task. We are also able to differentiate between 6 SN types with 60% accuracy given only two nights of data and 98% accuracy retrospectively.

1. Introduction

Supernovae are extremely bright explosions of stars that can rival the luminosity of an entire galaxy before fading away in just a few weeks. Current theories predict that supernovae are produced via two primary physical processes: gravitational collapse of the core of a massive star, and sudden re-ignition of nuclear fusion in a white dwarf. These different pathways produce SNe with different properties, which is encompassed in their type designation. Determining the type of observed SNe is particularly important in the case of type Ia SNe. Unlike other SN types, their standardizable

brightness makes them excellent distance indicators (or *standard candles*) on cosmological scales. Type Ia SNe were instrumental in the Nobel Prize-winning discovery of dark energy and the accelerating expansion of the universe (Perlmutter et al., 1999; Riess et al., 1998) and continue to be a crucial tool for further understanding the nature of dark energy and the composition of our universe.

Modern-scale sky surveys, including SDSS, Pan-STARRS, and the Dark Energy Survey, have identified thousands of supernovae throughout their operational lifetimes (Frieman et al., 2008; Chambers et al., 2016; Smith et al., 2020). However, it has been logistically challenging to follow up on most of these detections spectroscopically. The result is a small number of SNe with spectroscopically confirmed types and a large dataset of SN candidates with only observed brightness data in broad wavelength bands (*photometry*) and no type information. The upcoming Rubin Observatory Legacy Survey of Space and Time (LSST) is projected to discover 10^7 supernovae (LSST Science Collaboration et al., 2009), with millions of transient alerts awaiting classification each observing night. A reliable photometric classification algorithm will allow us to tap into the vast potential of the photometric dataset and pave the way for confident classification and analysis of the ever-growing library of transients from current and future sky surveys.

Given the scarcity of spectroscopic resources, the goal of this work is twofold: (1) confident retrospective classification of type Ia SNe using photometry alone in order to increase the number of cosmologically useful SNe, and (2) reliable real-time determination of SN type early in its lifetime to aid in optimal allocation of spectroscopic resources.

Our model produces both retrospective and real-time classification results with photometry data in the form of *light curves*, time-series data of observed brightnesses in multiple wavelength bands. Other deep learning approaches to this task include recurrent neural network-based SuperNNova (Möller & de Boissière, 2020) and RAPID (Muthukrishna et al., 2019), CNN-based PELICAN (Pasquet et al., 2019), and recurrent autoencoder-based SuperRAENN (Villar et al., 2020).

[1]Department of Physics and Astronomy, University of Pennsylvania, Philadelphia, PA 19104, USA [2]Centre for Astrophysics and Supercomputing, Swinburne University of Technology, 31122 Hawthorn, VIC, Australia [3]Université Grenoble Alpes, CNRS, LPSC-IN2P3, 38000 Grenoble, France. Correspondence to: Helen Qu <helenqu@sas.upenn.edu>.
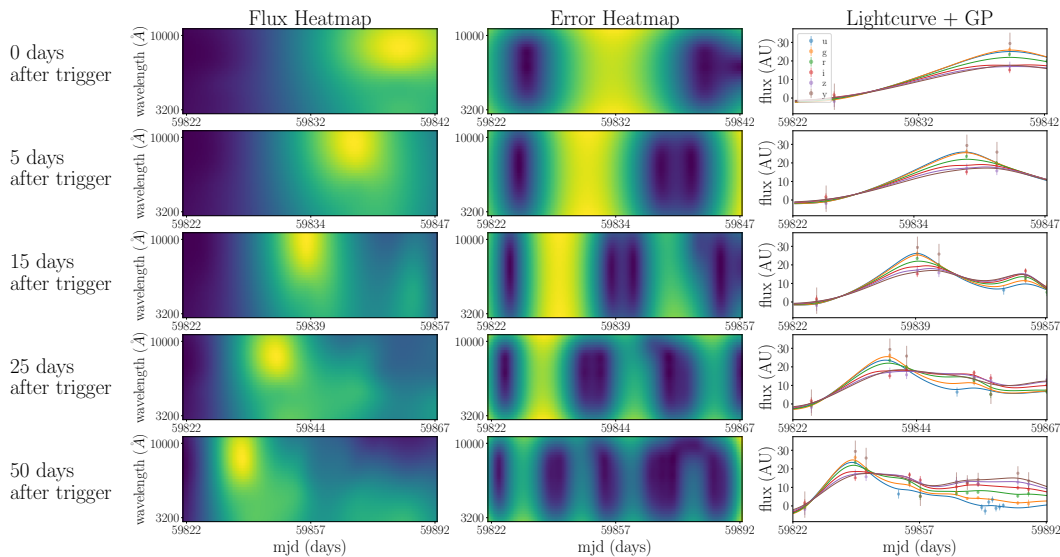
Figure 1. Flux and error heatmaps as well as lightcurves and Gaussian process fits of an SNII ($z = 0.39$) shown truncated at 0, 5, 15, 25, and 50 days after trigger. The flux and flux error measurements from the raw photometry are shown as points with error bars, while the Gaussian process fits to each photometry band are shown as curves.

2. Data

2.1. Datasets

This model was trained and evaluated on datasets created for the 2018 Photometric LSST Astronomical Time Series Classification Challenge (PLAsTiCC) (The PLAsTiCC team et al., 2018). All results were produced with a 80%/10%/10% training/validation/test split.

All lightcurves were observed in LSST's $ugrizY$ bands and realistic observing conditions were simulated using the LSST Operations Simulator (Delgado & Schumacher, 2014). We selected all type II, Iax, Ibc, Ia-91bg, Ia, and SLSN-1 supernova sources from this dataset and chose only supernovae in the well-sampled deep drilling fields. For binary (Ia vs. non-Ia) classification, the total source count is 12,611 after basic quality cuts on the sources: each source must have at least 5 detections, have cumulative signal-to-noise ratio at least 10, and have observations spanning at least 30 days.

The dataset used for type classification was created using the SuperNova ANAlysis package (SNANA) (Kessler et al., 2009) with the same parameters as the main dataset. 7,685 examples of each of the 6 types listed above were selected, making a full dataset size of 46,110 examples. To evaluate the model's real-time classification performance, five datasets were created from these simulations starting 20 nights prior to the date of trigger (t_{trigger}) and end at $N = 0, 5, 15, 25$, and 50 days after the date of trigger, respectively, where *trigger* is defined as the next observation exceeding a 5σ signal-to-noise detection threshold that occurs at least one night after the first.

2.2. Preprocessing

Prior to training, we preprocess our lightcurve data into 2-dimensional "images". First, all observations are labeled with the filter's central wavelength, calculated from the LSST filter transmission functions. We then follow Avocado (Boone, 2019) to apply 2-dimensional Gaussian process regression to the raw lightcurve data to model the event in the wavelength (λ) and time (t) dimensions. We obtain predictions from the trained Gaussian process model on a grid of λ, t values and call this our "image". The input to the model is the grid of Gaussian process predictions stacked depthwise with the Gaussian process prediction uncertainties at each λ, t, all normalized to the maximum flux value.

Figure 1 shows the raw lightcurve data, the Gaussian process model, and the resulting flux and uncertainty heatmaps for each of the real-time classification datasets.

3. Model

3.1. Base Model Architecture

The relatively simple architecture of our model, shown in Figure 2, allows for a minimal number of trainable parameters, speeding up the training process significantly without compromising on performance. It has a total of $\sim$ 22,000 trainable parameters when trained on images of size $32 \times 180 \times 2$ ($h \times w \times d$).

All convolutional layers in our model use full-height kernels, i.e. each convolutional layer has h filters and a kernel
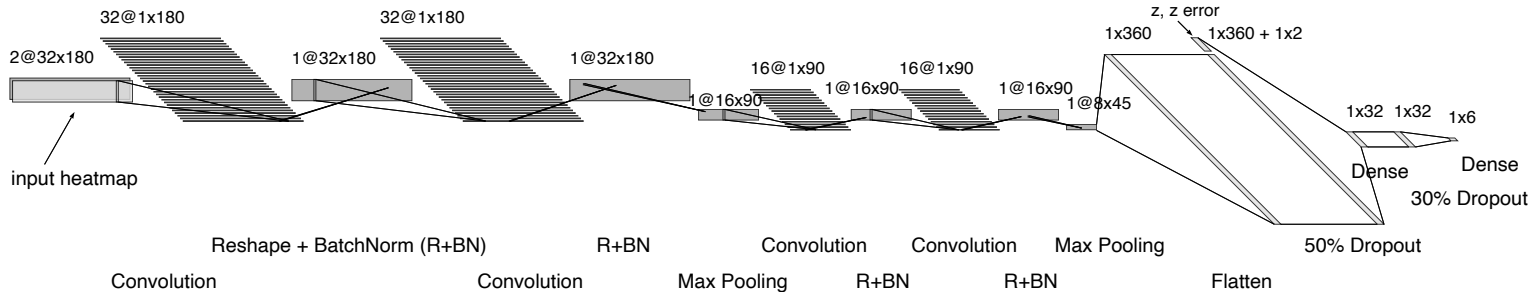
Figure 2. Model architecture with redshift information for real-time typing. The base architecture for retrospective binary classification does not include the redshift input (labeled z, z_{error}) and the output layer is replaced by a single sigmoid function.

size of $h \times 3$. This choice allows the model to learn from observations in all wavelengths simultaneously at every point in time. We reshape the resulting feature map to $h \times d \times 1$ to allow for further convolutions. The output layer is a single node for binary classification and 6 nodes for typing. Figure 2 shows the version for typing.

For all reported results, the model is trained with crossentropy loss and optimized with Adam (Kingma & Ba, 2017) at a constant 1e-3 learning rate for 400 epochs.

3.2. Model Architecture with Redshift

Cosmological redshift describes how quickly a light source is moving away from the observer, similar to the Doppler effect. Redshift is correlated with brightness and can help break degeneracies between types, but is not always available. To avoid relying on precise redshift estimates, all retrospective binary classification results are reported without redshift information. Real-time typing results are reported with and without redshift information.

The architecture of our model incorporating redshift and redshift uncertainty is shown in Figure 2. Spectroscopic redshift information is used when available, and photometric redshift estimates if not.

4. Results

4.1. Retrospective Classification

Our model achieves $99.73 \pm 0.26\%$ accuracy, $99.68 \pm 0.35\%$ precision, $99.78 \pm 0.22\%$ recall, and an AUC of 0.9994 on the Ia vs. non-Ia binary classification test dataset, prepared as described in Section 2.1. Figure 3 shows the confusion matrix, created with data from five independent runs of the classifier with a classification threshold of 0.5.

To simulate a more realistic classification scenario, our model was trained and evaluated on a dataset based on observed

Figure 3. Confusion matrix showing average and standard deviation over five runs for binary classification on the test set. The absolute numbers of examples are shown here as opposed to percentages.

abundances of each SN class and no class balancing was performed. The model still performs very well under these circumstances, as shown by the confusion matrix in Figure 5.

4.2. Real-Time Typing

Figure 4 shows the accuracy evolution over time for each supernova type in the test sets. The average classification accuracy across all 6 types starts at $\sim 60\%$ without redshift information on the night of trigger, and 75% with redshift. Redshift unequivocally improves classification performance, especially at early times when there is little photometric data to learn from. The largest improvement in accuracy occurred between 0 and 5 days after trigger for all datasets, likely due to the inclusion of the epoch of peak brightness.

4.3. Comparison to Existing Work

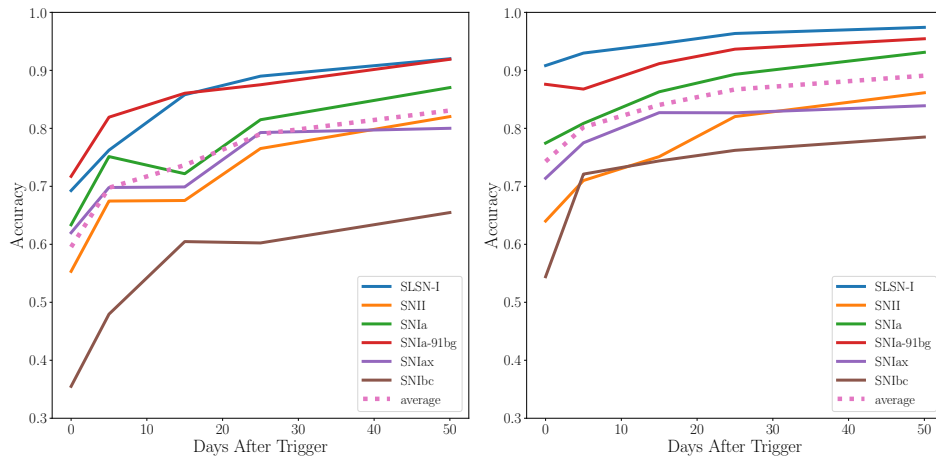SuperNNova (Möller & de Boissière, 2020) can classify SNe Ia vs. non-Ia with 99.55% accuracy training on a dataset

Figure 4. Accuracy/efficiency over time for each supernova type without redshift (top) and with redshift (bottom) for the $t_{\mathrm{trigger}} + N$ test datasets.

Figure 5. Confusion matrix showing average and standard deviation over five runs for SN typing on an imbalanced (realistic) dataset. The absolute numbers of examples are shown here as opposed to percentages.

of $\sim 900,000$ SNe with spectroscopic redshift information. However, our model achieves similar accuracy with just $\sim 12,000$ SNe and no redshift information. A closer comparison is a 92.4% accuracy achieved by SuperNNova trained with $\sim 50,000$ examples and no redshift information, which is noticeably worse than the results presented in this work.

SuperRAENN (Villar et al., 2020) is a semi-supervised model trained on real SN candidates, as opposed to the simulated observations used in this work. The most comparable result is shown in Figure 5 where the relative abundances of each SN type are based on real observations. The purity values achieved by our model are significantly higher for all the types shared by both works: 0.92 on SLSNe compared with 0.81, 0.993 on SNIa compared with 0.96, and

0.967 on SNIbc compared with 0.33.

RAPID (Muthukrishna et al., 2019) can differentiate between 12 transient types, including 7 supernova types, in real time. RAPID was tested on g and r band simulated data, as opposed to the $ugrizY$ bands available for simulations used in this work. Comparing our Figure 4, SCONE improves specifically upon RAPID's SNIbc and SNII classification accuracy. From Figure 7 of M19, 12% of SNIbc are correctly classified 2 days after detection, compared to SCONE's 54% accuracy at the date of trigger. 2 days after detection, SNII is classified at 7% accuracy by RAPID compared to 64% accuracy at the date of trigger by SCONE.

5. Conclusions and Future Work

We have presented a model addressing one of the most pressing problems in supernova science today: the lack of sufficient spectroscopic resources. Our model not only creates the opportunity for precision cosmology without spectroscopy by ensuring a pure dataset of Type Ia SNe using photometry alone, but also has demonstrated applicability to spectroscopic targeting with its real-time classification performance. The model is crucially able to perform these tasks with only 10^4 trainable parameters, making it lightweight and quick to train.

In future work, we would like to expand our model to classify other transient and variable phenomena. We are also interested in understanding and improving the out-of-distribution performance of the model, as data from simulatations often differs from real observations. Finally, since we rarely have accurate spectroscopic redshift information, we would like to evaluate the effect of incorrect redshift estimates on classification performance and its eventual impact on cosmological parameter estimates.

References

Boone, K. Avocado: Photometric classification of astronomical transients with gaussian process augmentation. *The Astronomical Journal*, 158(6):257, Dec 2019. ISSN 1538-3881. doi: 10.3847/1538-3881/ab5182. URL http://dx.doi.org/10.3847/1538-3881/ab5182.

Chambers, K. C., Magnier, E. A., Metcalfe, N., Flewelling, H. A., Huber, M. E., Waters, C. Z., Denneau, L., Draper, P. W., Farrow, D., Finkbeiner, D. P., Holmberg, C., Koppenhoefer, J., Price, P. A., Rest, A., Saglia, R. P., Schlafly, E. F., Smartt, S. J., Sweeney, W., Wainscoat, R. J., Burgett, W. S., Chastel, S., Grav, T., Heasley, J. N., Hodapp, K. W., Jedicke, R., Kaiser, N., Kudritzki, R. P., Luppino, G. A., Lupton, R. H., Monet, D. G., Morgan, J. S., Onaka, P. M., Shiao, B., Stubbs, C. W., Tonry, J. L., White, R., Bañados, E., Bell, E. F., Bender, R., Bernard, E. J., Boegner, M., Boffi, F., Botticella, M. T., Calamida, A., Casertano, S., Chen, W. P., Chen, X., Cole, S., Deacon, N., Frenk, C., Fitzsimmons, A., Gezari, S., Gibbs, V., Goessl, C., Goggia, T., Gourgue, R., Goldman, B., Grant, P., Grebel, E. K., Hambly, N. C., Hasinger, G., Heavens, A. F., Heckman, T. M., Henderson, R., Henning, T., Holman, M., Hopp, U., Ip, W. H., Isani, S., Jackson, M., Keyes, C. D., Koekemoer, A. M., Kotak, R., Le, D., Liska, D., Long, K. S., Lucey, J. R., Liu, M., Martin, N. F., Masci, G., McLean, B., Mindel, E., Misra, P., Morganson, E., Murphy, D. N. A., Obaika, A., Narayan, G., Nieto-Santisteban, M. A., Norberg, P., Peacock, J. A., Pier, E. A., Postman, M., Primak, N., Rae, C., Rai, A., Riess, A., Riffeser, A., Rix, H. W., Röser, S., Russel, R., Rutz, L., Schilbach, E., Schultz, A. S. B., Scolnic, D., Strolger, L., Szalay, A., Seitz, S., Small, E., Smith, K. W., Soderblom, D. R., Taylor, P., Thomson, R., Taylor, A. N., Thakar, A. R., Thiel, J., Thilker, D., Unger, D., Urata, Y., Valenti, J., Wagner, J., Walder, T., Walter, F., Watters, S. P., Werner, S., Wood-Vasey, W. M., and Wyse, R. The Pan-STARRS1 Surveys. *arXiv e-prints*, art. arXiv:1612.05560, December 2016.

Delgado, F. and Schumacher, G. The LSST OCS scheduler design. In *Society of Photo-Optical Instrumentation Engineers (SPIE) Conference Series*, volume 9149 of *Society of Photo-Optical Instrumentation Engineers (SPIE) Conference Series*, pp. 91490G, August 2014. doi: 10.1117/12.2056871.

Frieman, J. A., Bassett, B., Becker, A., Choi, C., Cinabro, D., DeJongh, F., Depoy, D. L., Dilday, B., Doi, M., Garnavich, P. M., Hogan, C. J., Holtzman, J., Im, M., Jha, S., Kessler, R., Konishi, K., Lampeitl, H., Marriner, J., Marshall, J. L., McGinnis, D., Miknaitis, G., Nichol, R. C., Prieto, J. L., Riess, A. G., Richmond, M. W., Romani, R., Sako, M., Schneider, D. P., Smith, M., Takanashi, N., Tokita, K., van der Heyden, K., Yasuda, N., Zheng, C., Adelman-McCarthy, J., Annis, J., Assef, R. J., Barentine, J., Bender, R., Blandford, R. D., Boroski, W. N., Bremer, M., Brewington, H., Collins, C. A., Crotts, A., Dembicky, J., Eastman, J., Edge, A., Edmondson, E., Elson, E., Eyler, M. E., Filippenko, A. V., Foley, R. J., Frank, S., Goobar, A., Gueth, T., Gunn, J. E., Harvanek, M., Hopp, U., Ihara, Y., Ivezić, Ž., Kahn, S., Kaplan, J., Kent, S., Ketzeback, W., Kleinman, S. J., Kollatschny, W., Kron, R. G., Krzesiński, J., Lamenti, D., Leloudas, G., Lin, H., Long, D. C., Lucey, J., Lupton, R. H., Malanushenko, E., Malanushenko, V., McMillan, R. J., Mendez, J., Morgan, C. W., Morokuma, T., Nitta, A., Ostman, L., Pan, K., Rockosi, C. M., Romer, A. K., Ruiz-Lapuente, P., Saurage, G., Schlesinger, K., Snedden, S. A., Sollerman, J., Stoughton, C., Stritzinger, M., Subba Rao, M., Tucker, D., Vaisanen, P., Watson, L. C., Watters, S., Wheeler, J. C., Yanny, B., and York, D. The Sloan Digital Sky Survey-II Supernova Survey: Technical Summary. , 135(1):338–347, January 2008. doi: 10.1088/0004-6256/135/1/338.

Kessler, R., Bernstein, J. P., Cinabro, D., Dilday, B., Frieman, J. A., Jha, S., Kuhlmann, S., Miknaitis, G., Sako, M., Taylor, M., and Vanderplas, J. SNANA: A Public Software Package for Supernova Analysis. , 121(883):1028, September 2009. doi: 10.1086/605984.

Kingma, D. P. and Ba, J. Adam: A method for stochastic optimization, 2017.

LSST Science Collaboration, Abell, P. A., Allison, J., Anderson, S. F., Andrew, J. R., Angel, J. R. P., Armus, L., Arnett, D., Asztalos, S. J., Axelrod, T. S., Bailey, S., Ballantyne, D. R., Bankert, J. R., Barkhouse, W. A., Barr, J. D., Barrientos, L. F., Barth, A. J., Bartlett, J. G., Becker, A. C., Becla, J., Beers, T. C., Bernstein, J. P., Biswas, R., Blanton, M. R., Bloom, J. S., Bochanski, J. J., Boeshaar, P., Borne, K. D., Bradac, M., Brandt, W. N., Bridge, C. R., Brown, M. E., Brunner, R. J., Bullock, J. S., Burgasser, A. J., Burge, J. H., Burke, D. L., Cargile, P. A., Chandrasekharan, S., Chartas, G., Chesley, S. R., Chu, Y.-H., Cinabro, D., Claire, M. W., Claver, C. F., Clowe, D., Connolly, A. J., Cook, K. H., Cooke, J., Cooray, A., Covey, K. R., Culliton, C. S., de Jong, R., de Vries, W. H., Debattista, V. P., Delgado, F., Dell'Antonio, I. P., Dhital, S., Stefano, R. D., Dickinson, M., Dilday, B., Djorgovski, S. G., Dobler, G., Donalek, C., Dubois-Felsmann, G., Durech, J., Eliasdottir, A., Eracleous, M., Eyer, L., Falco, E. E., Fan, X., Fassnacht, C. D., Ferguson, H. C., Fernandez, Y. R., Fields, B. D., Finkbeiner, D., Figueroa, E. E., Fox, D. B., Francke, H., Frank, J. S., Frieman, J., Fromenteau, S., Furqan, M., Galaz, G., Gal-Yam, A., Garnavich, P., Gawiser, E., Geary, J., Gee, P., Gibson, R. R., Gilmore, K., Grace, E. A., Green, R. F., Gressler, W. J., Grillmair, C. J., Habib, S., Haggerty, J. S., Hamuy, M., Harris, A. W., Hawley, S. L., Heavens, A. F., Hebb, L., Henry, T. J., Hileman, E., Hilton, E. J., Hoadley, K.,

Holberg, J. B., Holman, M. J., Howell, S. B., Infante, L., Ivezic, Z., Jacoby, S. H., Jain, B., R, Jedicke, R., Jee, M. J., Jernigan, J. G., Jha, S. W., Johnston, K. V., Jones, R. L., Juric, M., Kaasalainen, M., Styliani, Kafka, Kahn, S. M., Kaib, N. A., Kalirai, J., Kantor, J., Kasliwal, M. M., Keeton, C. R., Kessler, R., Knezevic, Z., Kowalski, A., Krabbendam, V. L., Krughoff, K. S., Kulkarni, S., Kuhlman, S., Lacy, M., Lepine, S., Liang, M., Lien, A., Lira, P., Long, K. S., Lorenz, S., Lotz, J. M., Lupton, R. H., Lutz, J., Macri, L. M., Mahabal, A. A., Mandelbaum, R., Marshall, P., May, M., McGehee, P. M., Meadows, B. T., Meert, A., Milani, A., Miller, C. J., Miller, M., Mills, D., Minniti, D., Monet, D., Mukadam, A. S., Nakar, E., Neill, D. R., Newman, J. A., Nikolaev, S., Nordby, M., O'Connor, P., Oguri, M., Oliver, J., Olivier, S. S., Olsen, J. K., Olsen, K., Olszewski, E. W., Oluseyi, H., Padilla, N. D., Parker, A., Pepper, J., Peterson, J. R., Petry, C., Pinto, P. A., Pizagno, J. L., Popescu, B., Prsa, A., Radcka, V., Raddick, M. J., Rasmussen, A., Rau, A., Rho, J., Rhoads, J. E., Richards, G. T., Ridgway, S. T., Robertson, B. E., Roskar, R., Saha, A., Sarajedini, A., Scannapieco, E., Schalk, T., Schindler, R., Schmidt, S., Schmidt, S., Schneider, D. P., Schumacher, G., Scranton, R., Sebag, J., Seppala, L. G., Shemmer, O., Simon, J. D., Sivertz, M., Smith, H. A., Smith, J. A., Smith, N., Spitz, A. H., Stanford, A., Stassun, K. G., Strader, J., Strauss, M. A., Stubbs, C. W., Sweeney, D. W., Szalay, A., Szkody, P., Takada, M., Thorman, P., Trilling, D. E., Trimble, V., Tyson, A., Berg, R. V., Berk, D. V., VanderPlas, J., Verde, L., Vrsnak, B., Walkowicz, L. M., Wandelt, B. D., Wang, S., Wang, Y., Warner, M., Wechsler, R. H., West, A. A., Wiecha, O., Williams, B. F., Willman, B., Wittman, D., Wolff, S. C., Wood-Vasey, W. M., Wozniak, P., Young, P., Zentner, A., and Zhan, H. Lsst science book, version 2.0, 2009.

Möller, A. and de Boissière, T. SuperNNova: an open-source framework for Bayesian, neural network-based supernova classification. , 491(3):4277–4293, January 2020. doi: 10.1093/mnras/stz3312.

Muthukrishna, D., Narayan, G., Mandel, K. S., Biswas, R., and Hložek, R. RAPID: Early Classification of Explosive Transients Using Deep Learning. , 131(1005):118002, November 2019. doi: 10.1088/1538-3873/ab1609.

Pasquet, J., Pasquet, J., Chaumont, M., and Fouchez, D. PELICAN: deeP architecturE for the LIght Curve ANalysis. , 627:A21, July 2019. doi: 10.1051/0004-6361/201834473.

Perlmutter, S., Aldering, G., Goldhaber, G., Knop, R. A., Nugent, P., Castro, P. G., Deustua, S., Fabbro, S., Goobar, A., Groom, D. E., Hook, I. M., Kim, A. G., Kim, M. Y., Lee, J. C., Nunes, N. J., Pain, R., Pennypacker, C. R., Quimby, R., Lidman, C., Ellis, R. S., Irwin, M., McMahon, R. G., Ruiz-Lapuente, P., Walton, N., Schaefer, B., Boyle, B. J., Filippenko, A. V., Matheson, T., Fruchter, A. S.,

Panagia, N., Newberg, H. J. M., Couch, W. J., and Project, T. S. C. Measurements of Ω and Λ from 42 High-Redshift Supernovae. , 517(2):565–586, June 1999. doi: 10.1086/307221.

Riess, A. G., Filippenko, A. V., Challis, P., Clocchiatti, A., Diercks, A., Garnavich, P. M., Gilliland, R. L., Hogan, C. J., Jha, S., Kirshner, R. P., Leibundgut, B., Phillips, M. M., Reiss, D., Schmidt, B. P., Schommer, R. A., Smith, R. C., Spyromilio, J., Stubbs, C., Suntzeff, N. B., and Tonry, J. Observational Evidence from Supernovae for an Accelerating Universe and a Cosmological Constant. , 116 (3):1009–1038, September 1998. doi: 10.1086/300499.

Smith, M., D'Andrea, C. B., Sullivan, M., Möller, A., Nichol, R. C., Thomas, R. C., Kim, A. G., Sako, M., Castander, F. J., Filippenko, A. V., Foley, R. J., Galbany, L., González-Gaitán, S., Kasai, E., Kirshner, R. P., Lidman, C., Scolnic, D., Brout, D., Davis, T. M., Gupta, R. R., Hinton, S. R., Kessler, R., Lasker, J., Macaulay, E., Wolf, R. C., Zhang, B., Asorey, J., Avelino, A., Bassett, B. A., Calcino, J., Carollo, D., Casas, R., Challis, P., Childress, M., Clocchiatti, A., Crawford, S., Frohmaier, C., Glazebrook, K., Goldstein, D. A., Graham, M. L., Hoormann, J. K., Kuehn, K., Lewis, G. F., Mandel, K. S., Morganson, E., Muthukrishna, D., Nugent, P., Pan, Y. C., Pursiainen, M., Sharp, R., Sommer, N. E., Swann, E., Thomas, B. P., Tucker, B. E., Uddin, S. A., Wiseman, P., Zheng, W., Abbott, T. M. C., Annis, J., Avila, S., Bechtol, K., Bernstein, G. M., Bertin, E., Brooks, D., Burke, D. L., Carnero Rosell, A., Carrasco Kind, M., Carretero, J., Cunha, C. E., da Costa, L. N., Davis, C., De Vicente, J., Diehl, H. T., Eifler, T. F., Estrada, J., Frieman, J., García-Bellido, J., Gaztanaga, E., Gerdes, D. W., Gruen, D., Gruendl, R. A., Gschwend, J., Gutierrez, G., Hartley, W. G., Hollowood, D. L., Honscheid, K., Hoyle, B., James, D. J., Johnson, M. W. G., Johnson, M. D., Kuropatkin, N., Li, T. S., Lima, M., Maia, M. A. G., March, M., Marshall, J. L., Martini, P., Menanteau, F., Miller, C. J., Miquel, R., Neilsen, E., Ogando, R. L. C., Plazas, A. A., Romer, A. K., Sanchez, E., Scarpine, V., Schubnell, M., Serrano, S., Sevilla-Noarbe, I., Soares-Santos, M., Sobreira, F., Suchyta, E., Tarle, G., Tucker, D. L., and Wester, W. First Cosmology Results using Supernovae Ia from the Dark Energy Survey: Survey Overview, Performance, and Supernova Spectroscopy. , 160(6):267, December 2020. doi: 10.3847/1538-3881/abc01b.

The PLAsTiCC team, Allam, Tarek, J., Bahmanyar, A., Biswas, R., Dai, M., Galbany, L., Hložek, R., Ishida, E. E. O., Jha, S. W., Jones, D. O., Kessler, R., Lochner, M., Mahabal, A. A., Malz, A. I., Mandel, K. S., Martínez-Galarza, J. R., McEwen, J. D., Muthukrishna, D., Narayan, G., Peiris, H., Peters, C. M., Ponder, K., Setzer, C. N., The LSST Dark Energy Science Collaboration, LSST Transients, T., and Variable Stars Science Collaboration.

The Photometric LSST Astronomical Time-series Classification Challenge (PLAsTiCC): Data set. *arXiv e-prints*, art. arXiv:1810.00001, September 2018.

Villar, V. A., Hosseinzadeh, G., Berger, E., Ntampaka, M., Jones, D. O., Challis, P., Chornock, R., Drout, M. R., Foley, R. J., Kirshner, R. P., Lunnan, R., Margutti, R., Milisavljevic, D., Sanders, N., Pan, Y.-C., Rest, A., Scolnic, D. M., Magnier, E., Metcalfe, N., Wainscoat, R., and Waters, C. SuperRAENN: A Semisupervised Supernova Photometric Classification Pipeline Trained on Pan-STARRS1 Medium-Deep Survey Supernovae. , 905 (2):94, December 2020. doi: 10.3847/1538-4357/abc6fd.